3D Printed Biomimetic Whisker-Based Sensor with Co-planar Capacitive Sensing

John Delamare, Remco Sanders and Gijs Krijnen
Robotics And Mechatronics group, University of Twente, Enschede, The Netherlands
Email: gijs.krijnen@utwente.nl

***Abstract* - This paper describes the development of a whisker sensor for tactile purposes and which is fabricated by 3D printing. Read-out consists of a capacitive measurement of a co-planar capacitance which is affected by a dielectric that is driven into the electric field of the capacitance. The current implementation contains a PCB to provide the required electrode structures. We present the design, fabrication and mechanical and capacitive characterisation of this sensor.**

Keywords - whisker; tactile sensor; 3D printed

I. Introduction

A. Rat Whisker

Rats are able to use their whiskers during exploration to extract information from objects in their near environment. They are able to determine various object features such as size, shape, texture, orientation, and location [1]. Around the base of the whisker shaft there are hundreds of neuro-receptors which detect the deflections of the whiskers, [2]. As such, tactile sensing using whisker offers several benefits, such as the ability to discern objects and the surrounds in an unlit environment. Moreover objects can be mapped without having to come in direct contact with the skin, which might be damaged due to direct contact depending on the properties of the object surface, e.g. imagine hot objects. In [3] it was proposed that whiskers may be used by rodents in a way analog to how some insects are supposed to use optical flow, i.e. an array of whisker sensors can provide a tactile flow signal based on the bending moment acting on the whiskers.

B. Approach

In this research project we attempt to develop a 3D printed passive whisker sensor, that is, without active whisking capability. The future aim is to integrate multiple sensing parts in the printed structure, e.g. by using doped fused deposition modeling (FDM) filament [4]. The proposed sensor should have 2 or more degrees of freedom with the intent to determine the contact force and its location along the whisker by measuring both force and moment at the whisker base. An advantage of this approach is the reduction in fabrication complexity and assembly with the added benefit that future versions may be easily extended to arrays of sensors and integrated in 3D printed robotics parts (embedded sensing).

Our work differentiates itself from prior work. Early papers on whisker based tactile sensing mostly concerned assembled structures, see e.g. [5]. A considerable number of papers is dedicated to what whisker sensors may contribute to robotics in terms of environmental awareness and navigation possibilties, see e.g. [6], but do not target the whisker sensor as such. In works like [7] the focus is on the reconstruction of surface texture rather than on the fabrication of whisker based sensors. The work reported in [8] makes use of commercial actuation and sensing units to implement active whisking and only the actual whiskers are 3D printed using a Digital Light Processing (DLP) based printer. The work in [9] and related papers is geared towards flow-sensing in water and the influence of specific whisker geometric attributes (undulations, curvature, etc.) but not at 3D printing of the actual sensors. Recently whisker sensors have been fabricated using 2D printing [10] but fully 3D printed sensors have been barely explored.

In this contribution we report the first developments of our approach to 3D print whisker based tactile sensors. We concentrate on the whisker structure and its base and investigate the possibility to measure rotations by placing the whisker model on a patterned printed circuit board (PCB), making use of the fringing fields of co-planar capacitances to measure the displacement of dielectric parts at the whisker base, see Fig. 1. The design of the capacitive read-out is analysed and mechanical and capacitive characterisation is reported.

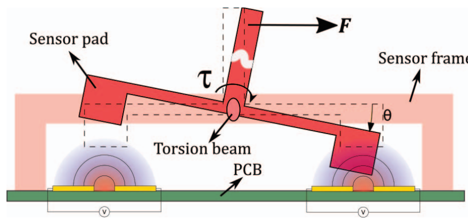

Fig. 1. Capacitive sensing using dielectrics driven into co-planar capacitors.

II. Methodology

A. Whisker

The base of the rat whisker can be modeled as a torsional spring in the event of initial object contact and boundary whisking [11]. Furthermore in order to increase the responsiveness of the system it should be critically damped and mechanically impedance matched [12]. Another factor which influences the responsiveness of the system is the distance between the rotating arm upon and the capacitor area [13]. The base structure chosen for this prototype is shown in Fig. 2.

In the design the whisker is supported by connecting it on both sides with elliptical bars allowing both for rotation (θ) and lateral displacement (x) of the whisker base. Eq. (1) and (2) describe the mechanics of the chosen whisker base structure when loaded by a force F_t at a distance a from the rotation axis:

$$m\ddot{x} + b_t\dot{x} + k_t x = F_t \tag{1}$$
$$J\ddot{\theta} + b_r\dot{\theta} + k_r\theta = F_t a \tag{2}$$

where m and J are the mass and moment of inertia of the whisker base structure, b_t and b_r the damping coefficient in transverse and rotational directions and k_t and k_r the spring constants for lateral and rotational directions. In statical situation these 2 equations allow for determination of both F_t and a from x and θ. The compliances of the beams are determined primarily by the beam length, cross-section, and the material properties. In the linear approximation the angular twist of an elliptical cross-section and the deflection of the bars are given by [14].

$$\theta = \frac{\tau L}{I_r G} \qquad\qquad x = \frac{F_t L_s^3}{6 E I_b} \tag{3}$$

where F_t and $\tau = F_t a$ are the force and moment acting on the whisker, G and E are the shear and Young's moduli, and I_r and I_b are the areal moments of inertia for torsion and bending.

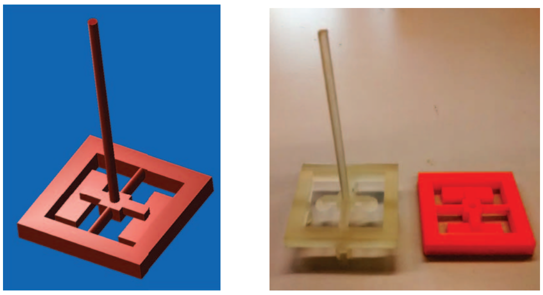

Fig. 2. Left: 3D CAD-design of whisker sensor in OpenScad [15]. Right: Printed whisker sensor (transparent, Veroclear) and base (red, PLA).

B. Printing

Due to the anisotropy of 3D printed layers print orientation has a considerable effect on the mechanical properties and in part determines the robustness of the structure [16]. In the design, the whisker is elongated vertically. If whiskers are printed with layers stacked vertically they will be susceptible to rupture when bent along the vertical axis. Thus when printing, ideally the structure should be printed at an angle which optimises the robustness of the whisker. The whisker structures were printed both on an Objet Eden 250 in Veroclear (resolution $16\,\mu\mathrm{m}$) as well as on an Ultimaker 2 in Poly Lactic Acid (PLA) (resolution of $100\,\mu\mathrm{m}$). In the latter case the whisker itself was not printed as part of the entire structure since only initial prototyping was concerned. The layers of the base structures were printed vertically as in preliminary prints the whiskers would have the tendency to fracture at the base. Further reported results are for the PLA whisker-base.

C. Capacitive Readout

The sensing part of the whisker sensor is based on changes in capacitance when a dielectric is driven into the field of a co-planar capacitance, see Fig. 1. The capacitive structure consist of a pattern of 23 interdigitated fingers of $0.2\,\mathrm{mm}$ width, $0.1\,\mathrm{mm}$ height, $3.6\,\mathrm{mm}$ length and with $0.4\,\mathrm{mm}$ space in between. Note that by choosing the ratio of electrode width to electrode spacing the sensitivity of the sensor for displacements of the dielectric can be taylored for a specific sensor design and printer choice.

In order to analyse the capacitance we applied various modelling approaches: a) an analytical method which only provides an order of magnitude approximation for the maximum achievable change in capacitance, b) a conformal mapping analysis [17] which allows to calculate the capacitance at intermediate positions of the dielectric and finally we used c) 2D Finite Element Method (FEM) calculations with periodic boundary conditions to numerically determine the capacitance versus distance curves (see Fig. 4).

III. Results

A. Displacement and rotation

In Fig. 3, top, displacements are plotted as function of the force exerted at the base of the whisker whereas Fig. 3, bottom, shows the measured and expected rotations versus moment for both increasing and decreasing load. The calculated trendlines are based on the expressions for I_b and I_r as found in [14] with PLA's Young's and shear moduli from [16].

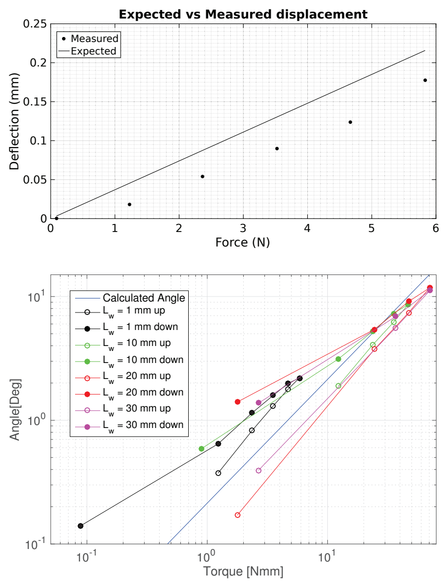

Fig. 3. Displacement (top) and rotation angle (bottom) versus load.

In the rotation angle measurements a clear hysteresis can be seen where the curve for decreasing moment shows larger rotational angles than the curve for increasing moment. Comparable hysteresis behaviour was observed for the deflection measurements. Other measurements, not shown here, also indicate creep of up to $1\,\mathrm{deg}$ for the torsional loading. Both creep and hysteresis are not uncommon for organic materials and generally pose problems. However, for the current whisker sensor which is based on differential measurements a high pass filter that filters out the low frequency drift components would help to suppress the creep related signals, but would not take care of the hysteresis. Depending on the type of information derived from the sensor this could require further improvement of the mechanical performance, e.g. by choosing different materials with lower creep and hysteresis such as nylon or acrylonitrile butadiene styrene (ABS).

B. Capacitive readout

Using an HP-4284A LCR meter and a linear translator the co-planar capacitance was determined and measured as a function of the separation between the interdigitated electrode pattern on the PCB and the dielectric pad of the whisker-sensor. Fig. 4 shows three measurement plots where the two curves measured at $1\,\mathrm{MHz}$ constitute a hysteresis curve. The same two plots display some odd behaviour at separation distances below $0.2\,\mathrm{mm}$ which we attribute to mechanical deformation of the dielectric pad and/or the PCB when mechanically loaded. Consequently we have shifted these curves $-0.2\,\mathrm{mm}$ to better reflect and compare them with the curve measured at $500\,\mathrm{kHz}$ and the two calculated curves. The maximum change

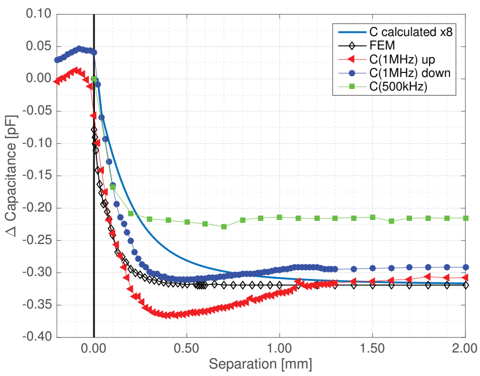

Fig. 4. Change in Capacitance versus displacement of the dielectric sensor pad, as calculated and measured

in capacitance is about $0.35\,\mathrm{pF}$ on a base value of about $2.1\,\mathrm{pF}$, i.e. $\Delta C/C \approx 0.17$. These values are well reflected in the FEM calculations but are under-estimated in the conformal mapping calculations by about a factor of 8.

It is interesting to note the increasing trend of the three measured plots starting around a separation gap of $0.6\,\mathrm{mm}$. Though the increase of capacitance in the absence of a dielectric substance is counter-intuitive this effect could be due to locations of certain grounded electrodes on the back of the PCB.

IV. Discusion and Conclusion

The design proposed in this paper is intended to function as a whisker which mimics that of rodents. The forces and moments at the whisker base are measured using the change of the co-planar capacitance sitting on a PCB. Focus was placed on testing the viability of the base structure. The model was designed with little freedom of motion for lateral displacement, and optimised for rotation by configuring the spring constants in the respective degrees of freedom.

Though the sensor was not characterised in its final shape one can predict its responsivity from the measurements presented in this paper which leads to a value of about $24\,\mathrm{N}^{-1}\,\mathrm{m}^{-1}$ for rotations smaller than $5\,\mathrm{deg}$.

Finally the capacitive structures potentially also can be used for electrostatic actuation, allowing the sensor to take advantage of active whisking. With the current design this would require about $8.5\,\mathrm{V}$ for $1\,\mathrm{deg}$ rotation which can be reduced by optimising the electrode pattern and reducing the torsional spring stiffness.

References

[1] J. A. Birdwell, J. H. Solomon, M. Thajchayapong, M. A. Taylor, M. Cheely, R. B. Towal, J. Conradt, and M. J. Hartmann, “Biomechanical models for radial distance determination by the rat vibrissal system,” *Journal of Neurophysiology*, vol. 98, no. 4, pp. 2439–2455, 2007.

[2] T. J. Prescott, M. J. Pearson, B. Mitchinson, J. C. W. Sullivan, and A. G. Pipe, “Whisking with robots from rat vibrissae to biomimetic technology for active touch,” *IEEE Robotics and Automation Magazine*, vol. 16, no. 3, pp. 42–50, 2009.

[3] C. L. Schroeder and M. J. Z. Hartmann, “Sensory prediction on a whiskered robot: A tactile analogy to ”optical flow”,” *Frontiers in Neurorobotics*, vol. 6, no. OCT, pp. 1–11, 2012.

[4] S. J. Leigh, R. J. Bradley, C. P. Purssell, D. R. Billson, and D. A. Hutchins, “A Simple, Low-Cost Conductive Composite Material for 3D Printing of Electronic Sensors,” *PLoS ONE*, vol. 7, no. 11, pp. 1–6, 2012.

[5] R. Russell, “Using tactile whiskers to measure surface contours,” *Proceedings 1992 IEEE International Conference on Robotics and Automation*, pp. 1295–1299, 1992.

[6] D. Jung and A. Zelinsky, “Whisker based mobile robot navigation,” *Proceedings of IEEE/RSJ International Conference on Intelligent Robots and Systems. IROS '96*, vol. 2, pp. 497–504, 1996.

[7] J. H. Solomon and M. J. Hartmann, “Biomechanics: robotic whiskers used to sense features.” *Nature*, vol. 443, no. 7111, p. 525, 2006.

[8] J. C. Sullivan, B. Mitchinson, M. J. Pearson, M. Evans, N. F. Lepora, C. W. Fox, C. Melhuish, and T. J. Prescott, “Tactile Discrimination Using Active Whisker Sensors,” *IEEE Sensors Journal*, vol. 12, no. 2, pp. 350–362, feb 2012.

[9] P. Valdivia Y Alvarado, V. Subramaniam, and M. Triantafyllou, “Design of a bio-inspired whisker sensor for underwater applications,” *Proceedings of IEEE Sensors 2012*, pp. 1–4, 2012.

[10] S. Harada, W. Honda, T. Arie, S. Akita, and K. Takei, “Fully printed, highly sensitive multifunctional artificial electronic whisker arrays integrated with strain and temperature sensors,” *ACS Nano*, vol. 8, no. 4, pp. 3921–3927, 2014.

[11] M. J. Hartmann, N. J. Johnson, R. B. Towal, and C. Assad, “Mechanical characteristics of rat vibrissae: resonant frequencies and damping in isolated whiskers and in the awake behaving animal,” *The Journal of neuroscience*, vol. 23, no. 16, pp. 6510–6519, 2003.

[12] H. Droogendijk, J. Casas, T. Steinmann, and G. Krijnen, “Performance assessment of bio-inspired systems: flow sensing mems hairs,” *Bioinspiration & biomimetics*, vol. 10, no. 1, p. 016001, 2014.

[13] N. Izadi, R. Jaganatharaja, J. Floris, and G. Krijnen, “Optimization of cricket-inspired, biomimetic artificial hair sensors for flow sensing,” *arXiv preprint arXiv:0802.3768*, 2008.

[14] W. C. Young and R. G. Budynas, *Roark's formulas for stress and strain*. McGraw-Hill New York, 2002, vol. 7.

[15] (2016). [Online]. Available: http://www.openscad.org

[16] J. Torres, J. Cotelo, J. Karl, and A. P. Gordon, “Mechanical Property Optimization of FDM PLA in Shear with Multiple Objectives,” *Jom*, vol. 67, no. 5, pp. 1183–1193, 2015.

[17] H. Da-Wei, C. Xin-Hong, W. Zhong-Jian, X. Da-Wei, S. Zhao-Rui, and Y. Yue-Hui, “An analytical model for coplanar waveguide on silicon-on-insulator substrate with conformal mapping technique,” *Chinese Physics B*, vol. 20, no. 1, p. 010210, 2011.